View metadata, citation and similar papers at core.ac.uk
brought to you by CORE
provided by Directory of Open Access Journals

T. RAMESHKUMAR, I. RAJENDRAN, A. D. LATHA

RESEARCH

Investigation on the Mechanical and Tribological Properties of Aluminium-Tin Based Plain Bearing Material

The purpose of this study is to investigate the Mechanical and Tribological properties of plain bearing alloys used especially in internal combustion engines. The mechanical properties namely Tensile strength and Hardness were investigated according to standard procedure. The sliding friction and wear properties of aluminium-tin alloy against high carbon high chromium steel were investigated at different normal loads as (29.43 N, 33.35 N and 36.25 N). Tests were carried in oil lubricated conditions with a sliding speed of 1 m/s. Prior to experimentation, the circulating engine oil 20w40 was heated to temperature of 80^0C using heater. The frictional behavior and wear property of aluminium-tin alloy were studied by means of pin-on-disk tribometer. The weight loss of the specimen was measured and wear and friction characteristics were calculated with respect to time, depth of wear track, sliding speed and bearing load. To determine the wear mechanism, the worn surfaces of the samples were examined using Scanning Electron Microscope (SEM). The optimum wear reduction was obtained at different normal loads and at same sliding speed.

Keywords: *Aluminium-Tin alloy, Pin-on-Disk Tribometer, Friction coefficient, Sliding wear, Hardness.*

1. INTRODUCTION

At the original equipment level, the use of aluminium in main and rod bearings is growing for a variety of reasons. One among them is, aluminium bearings are less expensive to manufacturer and it also gets rid of lead which is an environmental concern for manufacturers. Friction and wear occur to the machinery components which run together. The researchers investigate friction and wear behavior of materials because of the undesirable effect observed in the performance and life of machinery components [1].

T. Rameshkumar[1)], Dr I. Rajendran[2)] A. D. Latha[3)]
[1)]Department of Mechanical Engineering, Bannari Amman Institute of Technology, Sathyamangalam, Tamilnadu, India.
Email: t_rameshkumar2000@yahoo.com
[2)]Department of Mechanical Engineering, Dr Mahalingam College of Engineering & Technology, Pollachi,Tamilnadu, India.
Email: irajendran@drmcet.ac.in
[3)]Department of Mechanical Engineering, Nandha Engineering College, Perundurai, Tamilnadu, India.
Email: adlatha@yahoo.co.in

Aluminium alloys and other lightweight materials have growing applications in the automotive industry, with respect to reducing the fuel utilization and shielding the environment, where they can successfully reinstate steel and cast iron parts. These alloys are extensively used in buildings and constructions, containers and packaging, marine, aviation, aerospace and electrical industries because of their lightweight, corrosion resistance in most environments, or combination of these properties [2].

Aluminum alloys have higher conductivity (electrical and thermal) than most other metals, and they are usually cheaper than the alloys that are superior conductors (copper, silver, gold, etc.) [3]. Aluminium based alloy provides good combination of strength, corrosion resistance, along with fluidity and freedom from hot shortness [4]. According to Bowdon and Tabor, even in the existence of lubricant, metallic contact between the moving surfaces may readily occur, so that the basic functional properties of the alloys themselves are of primary importance [5].

Heniz leitner et al. [6] studied the characterization of mechanical properties of sliding bearing material

based on aluminium and reported that the static strength as well as the fatigue strength shows a strong dependence on temperature. Prasad Rao et al. [7] studied the improvement in tensile strength and load nearing capacity during dry wear of Al-7Si alloy combined grain refinement and modification.

Therefore, the purpose of this work was to investigate the microstructure, mechanical properties and lubricated friction, and wear behavior of locally produced Aluminium based alloys and to determine their most suitable chemical composition for tribological applications for plain bearings.

2. EXPERIMENTAL PROCEDURE

2.1 Preparation of alloys

The test specimen was prepared by using cladding process. In the process of cladding, metals are bonded with a thin layer of corrosion-resistant metal through the application of pressure, using rolls or other means. The lining thickness of the materials was measured by using Permascope. The maximum load carrying capacity of the bearing material is 29.06 MPa and the lining thickness of the aluminium based alloys is 600 μm.

2.2 Chemical composition of alloy and Pin Material

Aluminium based bearing alloys commonly contain tin (6-40%) as a soft component. Some of aluminium based bearing alloys contain silicon. It has very high hardness and its inclusions distributed over the aluminium matrix serve as an abrasive particle polishing the mating surface. Aluminum matrix of engine bearing alloys may be strengthened by addition of copper, nickel, chromium, manganese, magnesium, zinc etc.,

Here we chose pin material as shaft material, so we can study the appropriate wear characteristics for different conditions. The pin was AISI D3 (high carbon high chromium steel) material having a diameter of 5.041 mm and hardness range 720 BHN. The chemical composition of the pin and bearing material are given in the table 1. The pin material has high wear resistance with deep hardening properties. These characteristics are due to high content of chromium and carbon.

Table 1. Chemical composition of the bearing and pin material

Chemical Composition	
Aluminium-Tin based bearing material	Pin Material (High carbon High chromium Steel)
Sn 17.5-22.5% Cu 0.7-1.0% Si 0.7% max Fe 0.7% max Al rest of composition	C 2-2.5% Mn 0.25-0.3% Si 0.25-0.3% V 0.2% Mo 0.8% Fe remaining

2.3 Microstructure

The microstructures of the alloys were investigated using optical microscope. Figure 1 shows the microstructure of aluminium-based alloy. Here Tin is distributed in aluminium matrix as a separate phase in form of reticular (network) structure along the edges of aluminium grains. The bi-metal structure consisting of two layers: steel back and an aluminium-based alloy of about 0.6 mm thick.

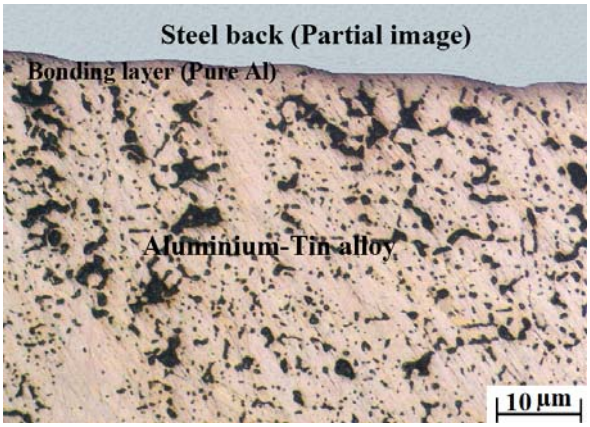

Figure 1. Microstructure of Al-Tin based alloy

2.4 Load calculations

Based on the product working conditions and available test machine capabilities, the wear test parameters, like sliding speed and load have been selected. The maximum load carrying capacity, sliding speed and the applied loads were shown in table 2. The maximum load to be applied at the end of the lever is determined by dividing the maximum load with the lever multiplication factor (15 to 17). The mean diameter of wear track was selected as 55 mm for a lever multiplication factor 16. The material was subjected to wear test at a constant sliding speed with different loads.

Parameters selected:

Pin diameter (d) = 5.041 mm

Track diameter = 55 mm

Pin area (A) = $(\pi \times d^2) / 4$
= $(\pi \times 5.041^2) / 4$
= 19.9583 mm²

Stress (σ) = 29.06 MPa (or)
29.06 N/mm^2

Max. Load to be applied = 29.06 x 19.9583
= 579.9882 N ≈ 580 N

Load multiplication factor = 16

Load to be applied at end = 580 /16 = 36.25 N

Table 2. Maximum load carrying capacity of the materials

Maximum load carrying capacity with multiplication factor, N	Applied loads with Multiplication factor, N			Sliding speed, m/s
	Load 1	Load 2	Load 3	
36.25	29.43	33.35	36.25	1

2.5 Physical and mechanical test results

The Tensile test is one of the most widely used tests to determine the mechanical properties of materials. In this test, a piece of material is pulled until it fractures. During the test, the specimen elongation and applied load is measured. Strain and stress are calculated from these values, and are used to construct a stress-strain curve. From this curve, the elastic modulus and yield strength are determined. The highest load in the tensile test gives the tensile or ultimate strength. After fracture, the final length and cross-sectional area of the specimen are used to calculate the percentage elongation and percent reduction of area, respectively. These quantities indicate the ductility of the material. The typical standard specimen is shown in fig 2.

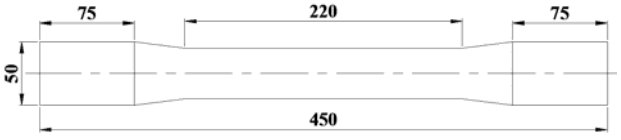

Figure 2. Tensile test specimen of standard IS:2102

The hardness of the materials was measured using Brinell hardness test. The materials were subjected to hardness test followed by tensile test. Brinell hardness was measured using a 5 mm of ball indenter at a load of 2500 N. The load was allowed to act for about 1 minute till the indicator comes to complete rest. The Brinell hardness number is calculated by dividing the load applied by the surface area of the indentation.

$$BHN = \frac{2F}{\pi D\left[D - \left(D^2 - D_1{}^2\right)^{1/2}\right]}$$

Here, D – Indenter diameter, and
D_1 – Indentation diameter

Before and after the friction and wear experiments, roughness measurements were conducted with the aid of a surface roughness tester (model: SJ-201P), in order to ensure that the specimens had similar surface morphology.

2.6 Description of test device

Pin-on-disc is the versatile equipment designed to study frictional and sliding wear process. The sliding occurs between a stationary pin and a rotating disc (Figure 3). The normal load to the pin can be varied from 196.2 to 1962 N weight. The maximum mean diameter of wear track is 74 mm. The disc speed can be set between 100 to 1200 rpm. The wear is measured through an LVDT (Linear Variable Displacement Transducer) and digital displacement monitor. The tangential frictional force is measured continuously through a 196.2 N load cell and a digital load indicator.

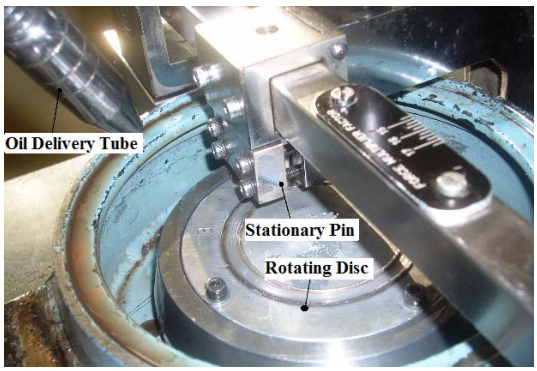

Figure 3. View of stationary pin & rotating disc

The lubricant pump can be started after filling its chamber with oil. The outlet of the pump is connected to a heating chamber. Its temperature can be set from ambient to 80°C using electronic indicating regulator. The oil delivery tube can be adjusted to deliver the oil close to the pin to ensure proper lubrication. The splash guard collects and returns the oil to the cooling chamber. The cooling coil of this chamber should be connected to the local water circulation system.

2.7 Material preparation

The material consists of two metal strips bonded together. One used for lining and the other for backing. Lining side usually, soft and directly, contacts with the other material whereas backing side consists of hard and stronger than lining side. Lining side consists of materials like aluminium, copper and lead for maximum fatigue strength. While the backing side usually made up of low carbon steel. Since the backing materials have high toughness, they also help in handling shock forces. Figure 4 shows the different layers used in aluminium-based alloy. The sheets of each material have been cut into 100mm size and processed as test specimen (Disc) i.e. the dimensions can be required by cutting, machining and drilling operations.

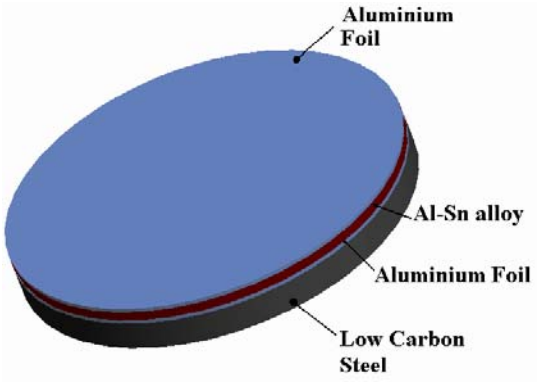

Figure 4. Layer of Al-Tin based alloy (100 mm)

3. RESULTS AND DISCUSSION

3.1 Mechanical test

The tensile test for the aluminium-tin alloy was carried out using Universal Testing Machine (UTM). Aluminium-tin alloy have relatively lower Young's modulus since the copper content is relatively low.

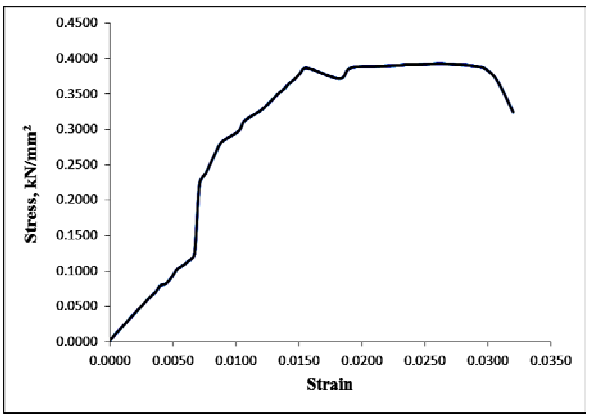

Figure 5. Stress-strain diagram for Aluminium-Tin alloy

From the figure 5 it infers the proportionality limit is low. This shows the low strength of the material. The graph shows that clear transition of elastic to plastic state which was used to locate yield point. The results were used to calculate the required properties such as yield strength, ultimate strength, permissible stress, Young's modulus and percentage of elongation, as tabulated below (Table 3).

Table 3. Results of Tensile test

Young's Modulus, N/mm^2	Yield Strength, N/mm^2	Ultimate Strength, N/mm^2	% of elongation
18663	130	397.6	3.3

The results obtained from hardness testing using Brinell Hardness Tester and the values are shown in Table 4. The resulting roughness of the aluminium-based alloy specimen was approximately 0.51 μm. Surface roughness value of bearing material values before and after wear test is shown in Table 5.

Table 4. Hardness of bearing materials

Materials	Al	Al-Tin Alloy
Hardness, HB	40	49

Table 5. Roughness value of bearing materials

Roughness	Al	Al- Tin Alloy
Before Wear, (μm)	3.16	0.51
After Wear, (μm)	4.92	2.11

3.2 Friction and wear test results

The successive recorded data were used for the quantification of both frictional behavior and wear of the sliding pairs. Accordingly, the relations concerning the actual friction coefficient and depth of wear were plotted as functions of the sliding distance in kilometres.

The readings in the graph were plotted at a regular interval of 30 minutes. Figure 6-9 indicates the wear (in microns) versus distance travelled (in km) for aluminium-based bearing alloy.

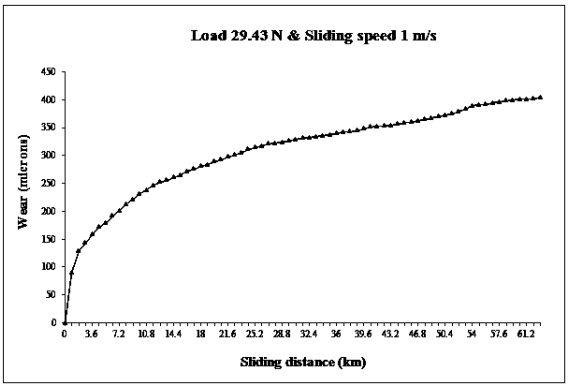

Figure 6. Time vs. displacement at load 29.43 N and 1 m/sec

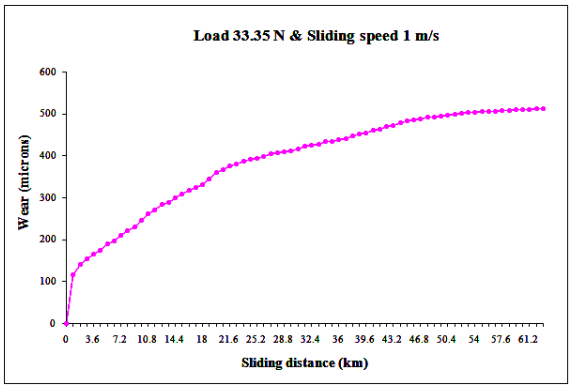

Figure 7. Time vs. displacement at load 33.35 N and 1 m/sec

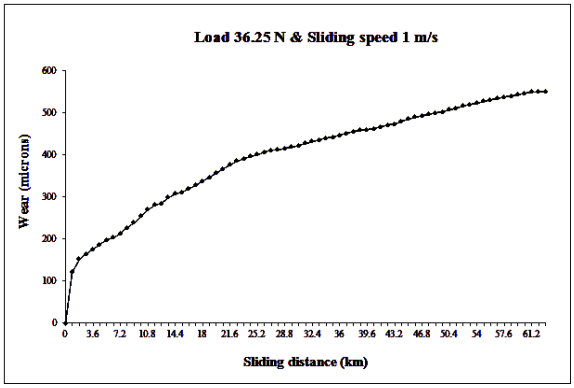

Figure 8. Time vs. displacement at load 36.25 N and 1 m/sec

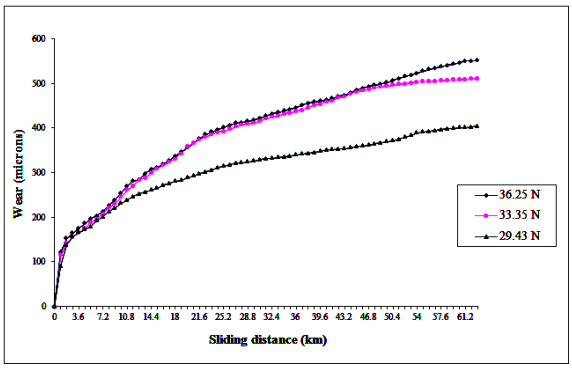

Figure 9. Time vs. displacement at loads 29.43, 33.35 and 36.25 N (1 m/sec)

Figures 10-13 show that initial wear is greater (upto 2.7 km). This is due to impact load at that time, and after that it gradually increases. We know that static friction is higher than dynamic friction [11] and this is also a reason for high initial wear. From the time of 2.7 km to 23.4 km, i.e., for next 20.7 km, the wear rate gradually increases, but it is very low compared to the initial wear rate. This is because of the hardness of aluminium-tin alloy. Since the asperities of the aluminium-tin alloy is in contact with the asperities of pin material (high carbon high chromium steel), the shape of asperities get changed. Initially the upper layer of asperities will be rough. Now after sliding contact, the rough surface is undergoing a transformation to form a relatively smooth surface.

From the time of 23.7 km to 61.2 km, i.e., for next 37.5 km, the wear is less, compared to that of previous 20.7 km. This indicates that the surface of asperities is getting smooth and relatively low frictional force is obtained. From the time of 61.2km to 63 km, i.e., for the next 1.8 km, the wear rate is very less. Because of the more contact area of surface of asperities has low frictional force. [10, 11]

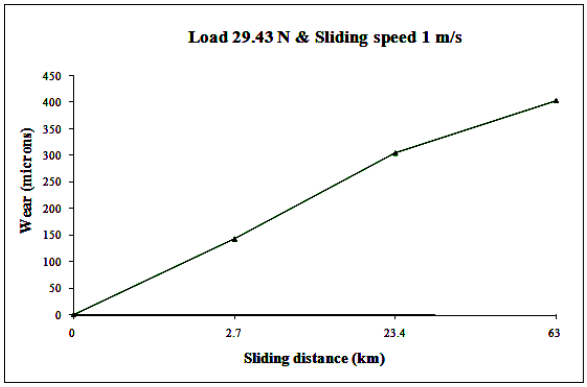

Figure 10. Time vs. displacement at load 29.43 N and 1 m/sec

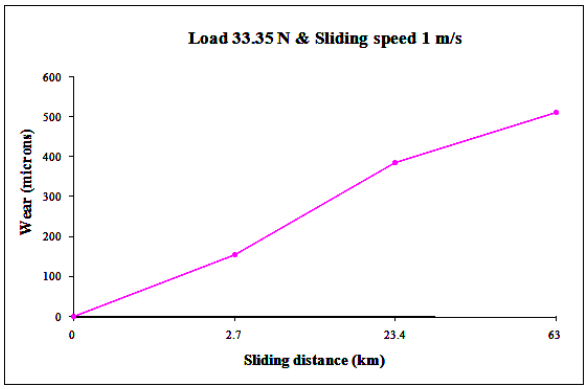

Figure 11. Time vs. displacement at load 33.35 N and 1 m/sec

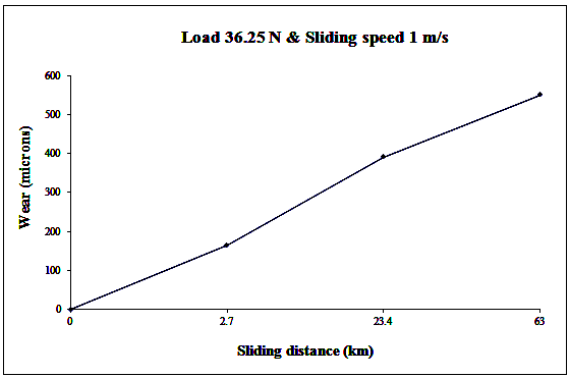

Figure 12. Time vs. displacement at load 36.25 N and 1 m/sec

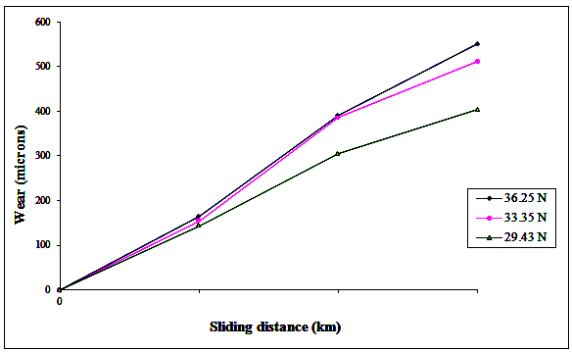

Figure 13. Time vs. displacement at loads 29.43, 33.35 and 36.25 N (1 m/sec)

Normally the bearing materials are compared in their working range (wear in microns). The values in table 6 are tabulated by comparing bearing material in their normal working range of 200 µm to 400 µm (wear).

Table 6. Working range of wear in bearing materials

Load, N	Working range of wear in bearing materials, 200 µm to 400 µm		
	200 µm	300 µm	400 µm
29.43	7.2 km	22.5 km	60.3 km
33.35	6.9 km	15.1 km	26.9 km
36.25	5.8 km	13.6 km	25.1 km

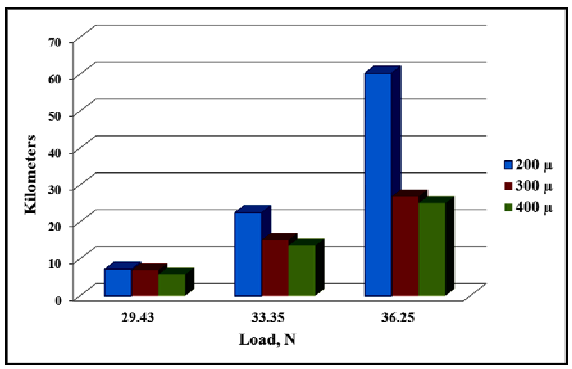

Figure 14. Load vs. kilometer of Aluminium-Tin based alloy

The values in the above tabulation are plotted in a chart, as shown in Figure 14.

The variation of the friction coefficient of the aluminium-based alloys as a function of sliding distance is shown in Figure 15-18. The friction coefficient of the alloys attained constant levels following an initial decrease.

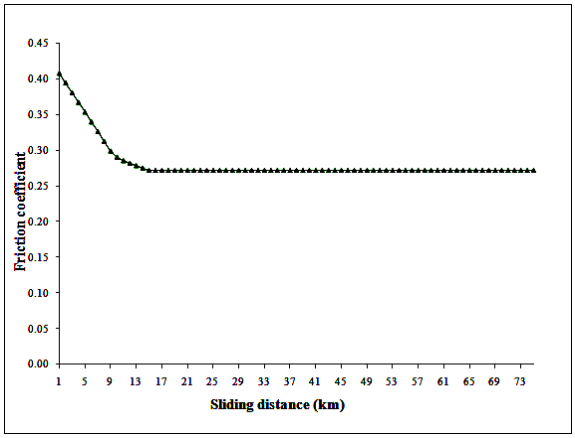

Figure 15. Time vs. friction coefficient at load 29.43 N and 1 m/s

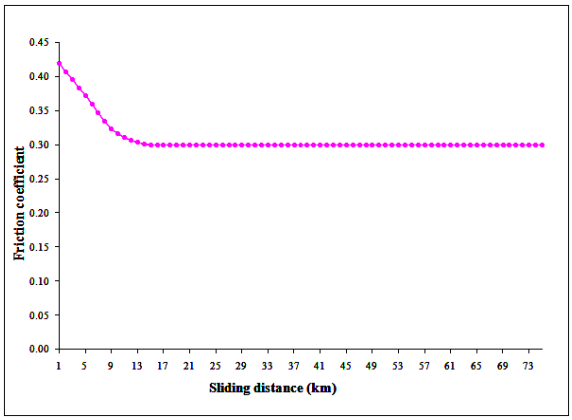

Figure 16. Time vs. friction coefficient at load 33.35 N and 1 m/s

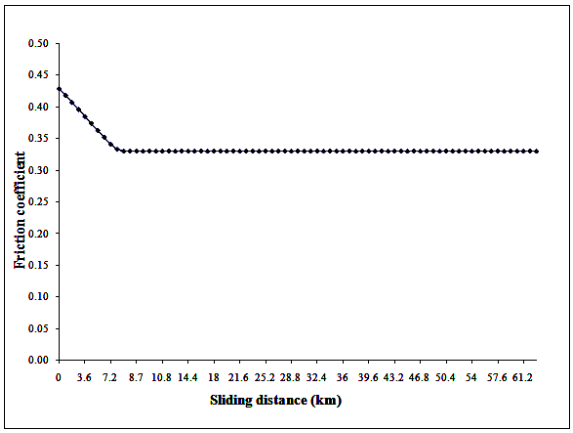

Figure 17. Time vs. friction coefficient at load 36.25 N and 1 m/s

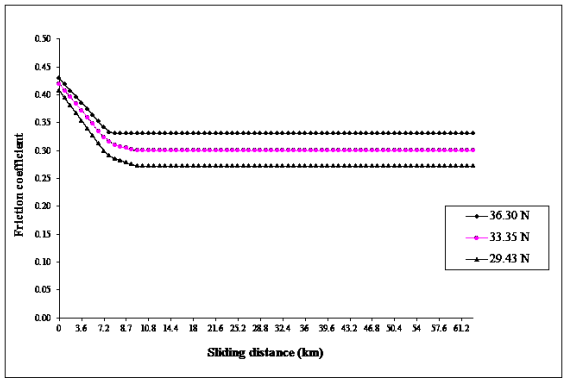

Figure 18. Time vs. friction coefficient at loads 29.43, 33.35 and 36.25 N (1 m/s)

Figure 19 shows that the friction coefficients of the applied load of 29.43 N were considerably smaller than those of the other two applied loads.

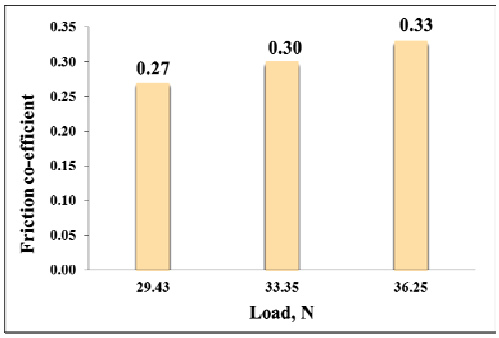

Figure 19. Load vs. friction coefficient 29.43 N, 33.35 N and 36.25 N and 1 m/s

The weights of the materials are measured before and after wear test. These values are tabulated in the table 7.

Table 7. Weight loss of the material

Load, N	Weight in grams		Weight loss, gms
	Before wear	After wear	
29.43	125.903	124.863	1.04
33.35		124.533	1.37
36.25		124.433	1.46

The Figure 20 shows that the weight loss of the material before and after the wear test at different normal loads 29.43, 33.35 and 36.25 N.

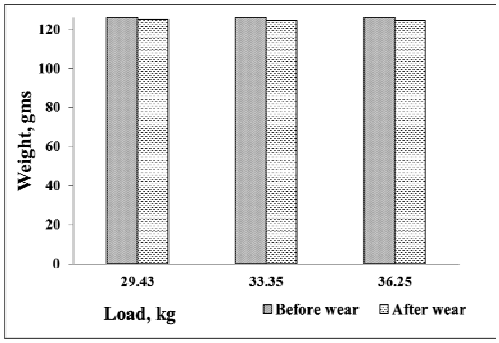

Figure 20. Comparison of weight before and after wear

3.3 Wear surface observations

The worn surfaces of the samples, obtained in test with the different loads and sliding speed of 1.0 m/s, are shown in figures 21-23. Surface projections or asperities present in the contact surface plastically deform and finally weld together by high local pressure in the relative motion between the contact surfaces. This suggests that the main wear mechanisms under these conditions are abrasive wear [12, 13].

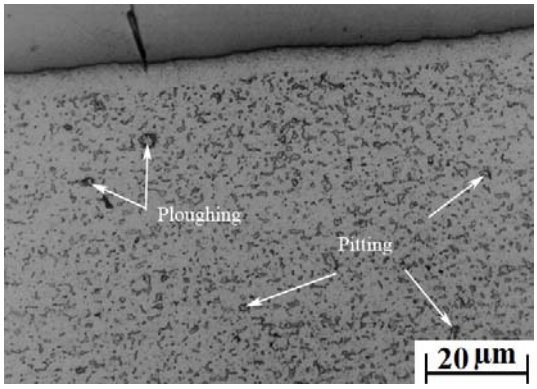

Figure 21. SEM micrographs of disc worn surface at 29.43 N and 1 m/sec

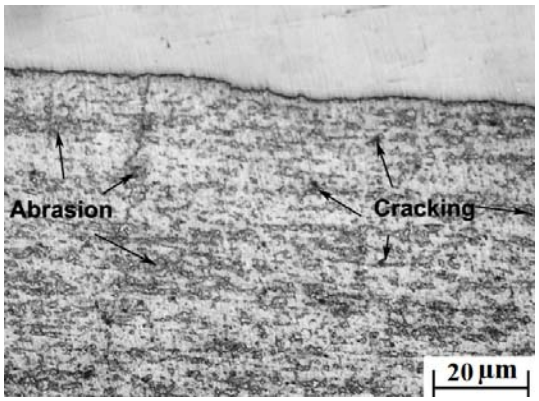

Figure 22. SEM micrographs of disc worn surface at 33.35 N and 1 m/sec

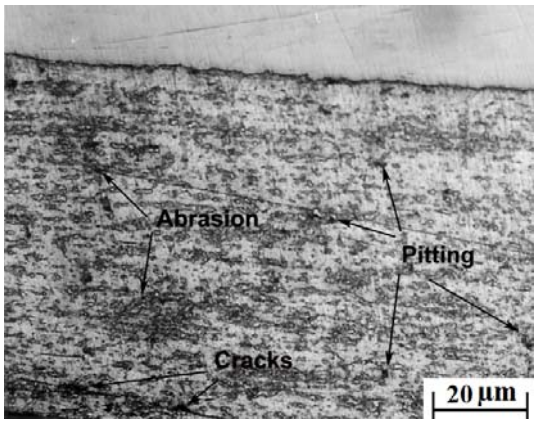

Figure 23. SEM micrographs of disc worn surface at 36.25 N and 1 m/sec

As the sliding continues, these bonds break up and produce micro cavities which cause tiny particle abrasion. In addition to these wear processes, corrosion also takes place in the specimen surface. These phenomena are supposed to be connected with the growth and progress of pits. The presence of micro cracks on the sliding surface is another important observation.

4. CONCLUSION

The aluminium-tin based alloy material may be effectively used in the industry due to better tribological properties like good resistance to corrosion, adequate strength, better surface properties and high fatigue strength. In this experiment, friction coefficient and wear test for aluminium-tin based bearing materials with three different loads were tested, using pin-on-disc apparatus, under oil lubricated conditions. The friction coefficient, wear and weight loss for three different loads were tabulated and their readings were plotted. From these the following conclusions were drawn.

1. Hardness values increased with addition of alloying element (1.225 times more than the pure aluminium)
2. The wear characteristics of bearing materials are compared in their working range of 200 μm to 400 μm with different normal loads.
3. Friction coefficient of aluminium-based alloy bearings is less than that of pure aluminium bearing.
4. Aluminium-based alloy bearings materials exhibit less wear compared to pure aluminium bearing.
5. The main wear mechanism of the aluminum alloy was due to plastic deformation and abrasion.

REFERENCES

[1] Bhushan: *Principles and Applications of Tribology*, John Wiley and Sons, USA, 1999.

[2] D.K. Allen: *Metallurgy theory and practice*, American technical society, Chicago (ASM), 1983.

[3] Kenneth G.Budinski, Michael K.Budinski: *Engineering Materials: Properties and Selection*, Prentice Hall of India Ltd., 2006

[4] Metals Handbook: *Properties and selection of Non-ferrous alloys and pure metals*, American society of metals (ASM), USA, 1979.

[5] F.P. Bowden and D. Tabor: *The Friction and Lubrication of Solids*, Oxford University Press, Oxford, 1954.

[6] Heniz Leitner, Istvan Godor and Christian Forstner: *Characterisation of the mechanical properties of sliding bearing materials based on Aluminium*, 2002.

[7] A.K. Prasad Rao, B.S. Murty, and M. Chakraborty: *Improvement in tensile strength and load bearing capacity during dry wear of Al-7Si alloys by combined grain refinement and modification*, materials science Engineering A395, pp 323-326, 2004.

[8] T. Rameshkumar, I. Rajendran: *A study on Tribological Behavior of Aluminium-Based Bearing Material in oil Lubricated Conditions*, National conference on Optimization Techniques in Engineering Science and Technology (OPTEST 2009), Bannari Amman Institute of Technology, Sathyamangalm, pp 20-21, 2009.

[9] T. Rameshkumar, I. Rajendran: *Failure Analysis of Carbon Chromium Steel (15cr65) Bearing*, International Conference on Recent Trends in Materials and Mechanical Engineering (ICMME 2008), Dr Mahalingam College of Engg. & Tech., Pollachi, pp 336-346, 2008.

[10] Prasanta Sahoo: *Engineering Tribology*. Prentice Hall of India Pvt., Ltd., New Delhi, 2005

[11] B.C.Majumdar: *Introduction to Tribology of Bearings,* Wheeler Publishing, 1999.

[12] R.Bowen, D.Scott, W.Seifert, V.C.Wescott: *Ferrography*, Tribology International, 9, 3, 1976, 109-115.

[13] S.Raadnui: *Wear particle analysis – utilization of quantitative computer image analysis, A Review,* Tribology International, 38, 10, 2005, 871-878.